Bulletin of the Seismological Society of America, Vol. 92, No. 2, pp. 711–722, March 2002

Ⓔ

Equivalent Medium Parameters for Numerical Modeling in Media with Near-Surface Low Velocities

by Leo Eisner* and Robert W. Clayton

Abstract We have developed a methodology to discretize an isotropic velocity model with low velocities near the free surface for full waveform numerical modeling. The method modifies the near-surface minimum velocity in a given (original) model by replacing parts of the model with equivalent medium parameters (EMP). The discretized model (with EMP) has a higher minimum velocity and minimizes the difference between the seismograms evaluated for the original model and the model with EMP. The method is suitable for studies requiring full waveform numerical modeling with a limited frequency range (such as a finite-difference full waveform modeling in a sedimentary basin). The discretized model with EMP is set to match locally surface-wave velocities evaluated in the original model over the frequency range of interest. The difference in group velocity calculated for the original vertical profile and the vertical profile with EMP provides an estimate of the error due to the modification of the original model.

Online material: source code for the discussed algorithm.

Introduction

Numerical solution of the wave equation has become practical for large heterogeneous models. The accuracy of the numerical simulations (i.e., the mesh size) is determined by the slowest velocities in the model, which may span only a small portion of the model (usually the shallow sediments at or near the surface). The computational time of the required numerical simulations increases with a smaller mesh size (the required computational time for a 3D finite-difference simulation [Graves, 1996] increases proportional to the fourth power of one over the mesh size). A simple clamping of the minimum velocities known as a velocity cutoff (e.g., Olsen *et al.,* 1995, 1997; Olsen and Archuleta, 1996; Graves, 1998; Wald and Graves, 1998; Olsen, 2000; for the definition used in this article, see the following paragraphs) can cause some significant errors, which appear to contaminate the surface waves. The velocity clamping often eliminates the near-surface structure, where many multiply reflected waves interfere constructively to create a significant effect on dispersion of long-period surface waves. Although attenuation will generally reduce the effect of the near-surface low-velocity structure, it does not eliminate it.

One solution to this problem is to use a variable mesh size to reduce the number of calculations while preserving the accuracy (Moczo *et al.,* 1997; Komatitsch and Tromp, 1999; Opršal and Zahradník, 1999). However, accurate variable mesh-size algorithms may substantially increase the computational complexity (Moczo *et al.,* 1997; Opršal and Zahradník, 1999) or mesh-generating algorithms (Komatitsch and Tromp, 1999). In this study, we propose a method in which the low-velocity regions are modified in a manner that is consistent with the surface-wave dispersion but allows coarser sampling of the medium. We do not include in our method attenuation of the low-velocity regions as it is beyond the scope of this article. We address how to sample models for elastic-wave propagation in isotropic media.

The problem of correct discretization and velocity clamping is more significant than is commonly realized, particularly in the calculation of the multiply reflected waves inside sedimentary basins. Graves (1997) made a simple attempt to see the effect of the velocity clamping by comparing synthetic seismograms computed for models with different values of the velocity clamping. Our analysis started with analogous numerical experiments in which we compared seismograms computed for models with different values of the velocity clamping. In these tests, a velocity clamped to a certain threshold replaces all velocities lower than that threshold. In the following, we refer to such a model as a clamped model. Figure 1 shows the effect of velocity clamping on long-period seismic-wave propagation. The direct body waves are not significantly affected, but later arrivals are very sensitive to the value of the velocity clamping. Both the source and the receiver are situated outside the sedimentary basins. Stations situated inside the sedimentary basin

*Present address: Schlumberger Cambridge Research, High Cross, Madingley Road, Cambridge, CB12PR, U.K.

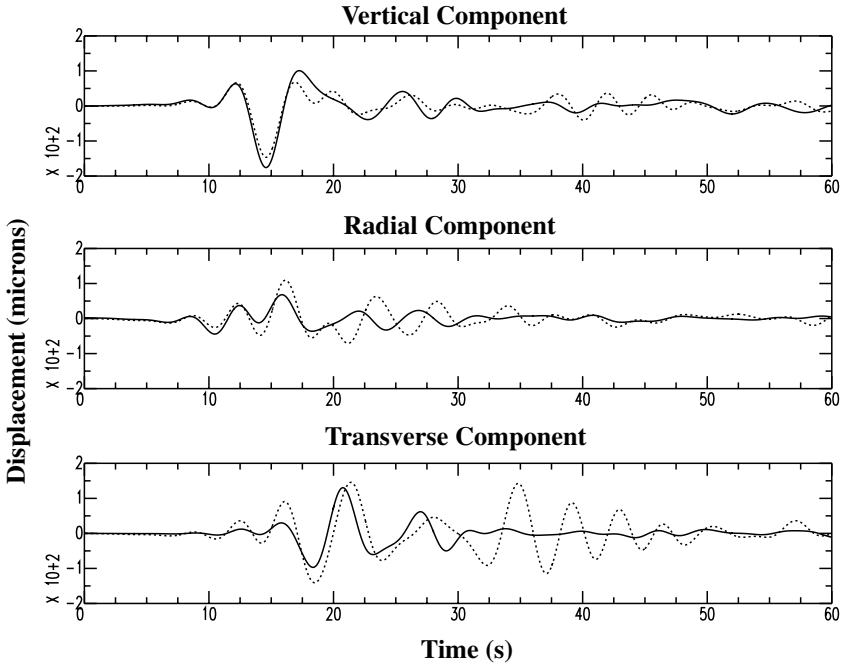

Figure 1. A comparison of synthetic seismograms computed for different values of the velocity clamping. Three components of displacement (in μm) due to a source in the model of SCVM (Version 1, Magistrale *et al.,* 1996). The event simulates an aftershock of the Landers earthquake (34.38° N, 118.49° W, and depth at 6.7 km) as recorded at station PAS (34.14° N, 118.17° W). The point-source double-couple mechanism of the aftershock has strike 278°, dip 56°, rake 63°, and moment 4.2. The solid line represents the displacement computed for a model with a minimum velocity clamped to 1.0 km/sec, and the dashed line represents the displacement computed for a model with a minimum velocity clamped to 0.5 km/sec. The velocity model includes strong lateral variations of both *P*- and *S*-wave velocities as well as density due to the presence of deep basins (Los Angeles and San Fernando in this case), however, neither source nor receiver is situated in the sedimentary basin. The results with no velocity clamping are not available because of extremely high numerical cost of such a simulation. All seismograms were low-pass filtered for periods longer than 3 sec.

show even more sensitivity to the value of the velocity clamping. The horizontal components are most severely affected, especially the transverse component, which is dominated by the Love waves.

We propose to discretize the original model in a way that preserves the surface-wave velocities. First we show the algorithm for a 1D model, and in the following section we generalize the algorithm for a 3D heterogeneous model. Finally, we test the algorithm with the numerical modeling of seismic waves in isotropic media. In the following, we refer to the input model as the original model, and the modified model is called the equivalent medium parameter (EMP) model.

Equivalent Medium Parameters for a 1D Vertical Profile

In this section we show how, for a given frequency range and a 1D vertical profile of medium parameters (in the following we refer to it as a vertical profile), we find an EMP vertical profile such that all synthetic seismograms (including surface waves) computed for both vertical profiles agree as closely as possible. We require two conditions to reduce the cost of numerical modeling: the minimum velocity in the modified vertical profile must be higher than a certain *a priori* selected threshold ($v_{\min}$), and the original and modified profiles are isotropic.

An analogous problem was solved by Backus (1962), who showed how to replace thin isotropic elastic layers with a homogeneous anisotropic layer. This method was generalized by Schoenberg and Muir (1989) for an arbitrary anisotropic elastic medium. This method is not dependent on the period range of interest (it is derived for infinitely long period), and the modified vertical profile is always anisotropic, and its minimum velocity may be lower than the *a priori* selected threshold.

Algorithm for a 1D Vertical Profile

The original 1D vertical profile of isotropic medium parameters is described by depth-dependent *P*-wave and *S*-wave velocities and density. The values of medium parameters in the original profile can be either continuous or

discrete. Let us assume there is a maximum depth h for which the *S*-wave velocity is lower than the *a priori* selected threshold. To modify the vertical profile, we evaluate the Love-wave group velocities $v_{\mathrm{gL}}^{\mathrm{or}}(T)$ over a range of periods of interest (T_1, T_2) using the original vertical profile. Then we find a new *S*-wave velocity and density EMP profile such that the *S*-wave velocity of the EMP profile is greater than or equal to the *a priori* selected threshold by minimizing the relative error of the Love-wave group velocities between the EMP and the original vertical profiles. We set the EMP vertical profile equal to the original vertical profile everywhere, except the top layer of thickness H, where H is greater than h. The EMP profile is then found by a gradient search for the three parameters of the top homogeneous layer of the EMP profile: the thickness H, the *S*-wave velocity $v_{\mathrm{s}}^{\mathrm{EMP}}$, and the density ρ^{EMP} To find the new parameters of the homogeneous layer ($H, v_{\mathrm{s}}^{\mathrm{EMP}}$, and ρ^{EMP}), we minimize

$$E = \underset{(T_1,T_2)}{L_1}\left[\frac{v_{\mathrm{gL}}^{\mathrm{EMP}}(T,H,v_{\mathrm{s}}^{\mathrm{EMP}},\rho^{\mathrm{EMP}}) - v_{\mathrm{gL}}^{\mathrm{or}}(T)}{v_{\mathrm{gL}}^{\mathrm{or}}(T)}\right]. \qquad (1)$$

Here the L_1 norm is applied over the period range of interest, and $v_{\mathrm{gL}}^{\mathrm{EMP}}(T,H,v_{\mathrm{s}}^{\mathrm{EMP}},\rho^{\mathrm{EMP}})$ is the group velocity evaluated from the EMP model.

The *P*-wave velocity is determined after we find the other parameters of the homogeneous layer: H, $v_{\mathrm{s}}^{\mathrm{EMP}}$, and ρ^{EMP}. We do not modify the *P*-wave velocity of the original model for depths greater than H. Ideally the *P*-wave velocity of the homogeneous layer should be determined by minimizing

$$E = \underset{(T_1,T_2)}{L_1}\left[\frac{v_{\mathrm{gR}}^{\mathrm{EMP}}(T,v_{\mathrm{p}}^{\mathrm{EMP}}) - v_{\mathrm{gR}}^{\mathrm{or}}(T)}{v_{\mathrm{gR}}^{\mathrm{or}}(T)}\right], \qquad (2)$$

where v_{gR} is the group velocity of Rayleigh waves, and $v_{\mathrm{p}}^{\mathrm{EMP}}$ is the *P*-wave velocity of the homogeneous layer in the EMP profile. However, for large 3D velocity models, evaluation of this equation is expensive (a gradient search). We found it to be sufficiently accurate to determine the *P*-wave velocity by using the ratio

$$\Re = \frac{1}{H}\int_0^H \frac{\lambda(z)}{\mu(z)}\mathrm{d}z,$$

where z is the depth and $\lambda(z)$ and $\mu(z)$ are uniquely determined from the medium parameters of the original vertical profile. The *P*-wave velocity for a homogeneous layer is then evaluated by

$$v_p^{EMP}(z_m) = v_{\mathrm{s}}^{\mathrm{EMP}}(z_{\mathrm{m}})\sqrt{\frac{\lambda+2\mu}{\mu}} = v_{\mathrm{s}}^{\mathrm{EMP}}(z_{\mathrm{m}})\sqrt{\Re+2}.$$

Figure 2 shows a flow chart of the previously described algorithm. The grid search over *S*-wave velocities and densities can be replaced with a gradient search.

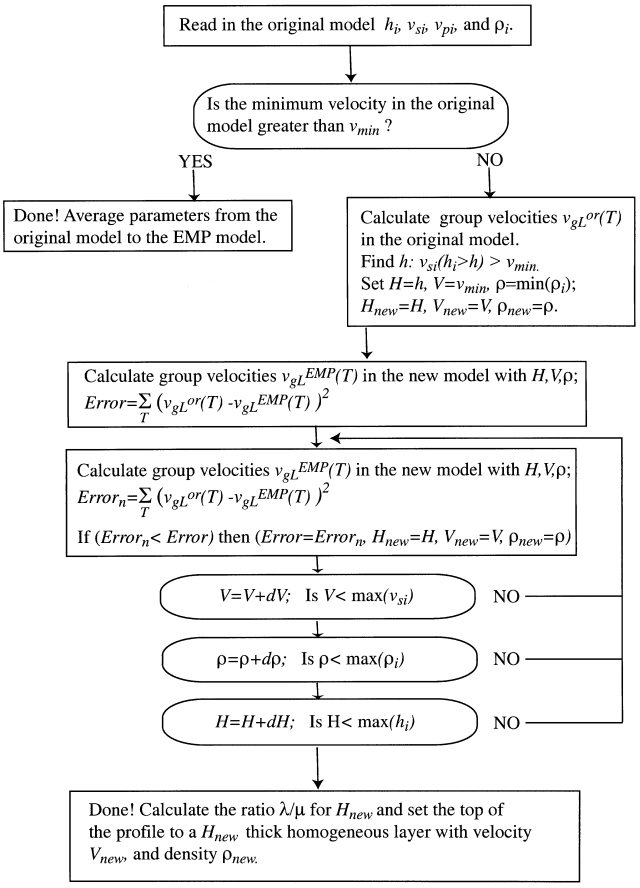

Figure 2. Flow chart of the equivalent medium parameter algorithm for a 1D profile.

Figure 3 illustrates the method of fitting the Love-wave dispersion with the equivalent medium parameters. The Love-wave group velocities from the EMP and the original vertical profiles match only over the frequency range of interest. Note that the group and phase velocities of the shorter periods are significantly different.

Discussion of the Algorithm for a 1D Vertical Profile

The lowest velocities in most models occur near the surface, and in our numerical experiments, we have found that Love waves are generally the most sensitive to the low-velocity structure near the surface. For this reason and for the reasons discussed in the Introduction we have based our algorithm on matching the Love waves rather than Rayleigh waves or body waves. Love waves in a 1D medium exist only on the transverse component. The frequency spectrum of the transverse component due to a source with a small frequency range in a vertically varying medium can be evaluated from the formula (7.147) of Aki and Richards (1980). That formula describes the elastic-wave propagation effects on the synthetic seismograms as a function of the depth of the source and the receiver. The elastic-wave propagation effects on the synthetic seismograms due to the horizontal

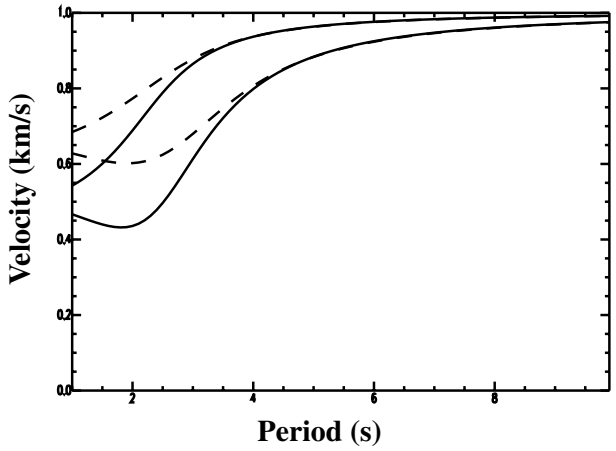

Figure 3. A comparison of the group and phase velocities of the original and the EMP models. The Love-wave group and phase dispersion is matched only in the frequency range of interest ($T > 3$ sec). The solid line represents group and phase velocity of the original model, and the dashed line represents the group and phase velocity of the EMP model (phase velocity is greater than or equal to group velocity in each model).

(epicentral) distance of the source and receiver of a finite-frequency signal centered at frequency ω_0 can be approximated by formula (7.11) of Aki and Richards (1980):

$$f_0(x,t,\omega_0) \sim \frac{\Delta\omega}{\pi}\frac{\sin Y}{Y}\cos\left[\omega_0\left(t-\frac{x}{c}\right)\right],$$

where $Y = \Delta\omega/2[t - x/v_g]$. Here $f_0(x, t)$ is a signal due to a normalized harmonic source of an angular frequency ω_0 at time t and distance x. The phase and group velocities of Love waves are c and v_g, respectively, both of which are functions of ω_0.

Because we modify the original model, we cannot obtain exactly the same seismograms computed for the original and the EMP models. An exact match between the seismograms computed for the two models would mean we match exactly the eigenfunctions and the group and phase velocities evaluated at the original and the EMP models for the frequency range of interest, which is not possible. We have the choice of matching the phase velocities, the group velocities, or the eigenfunctions evaluated for the original and the EMP models. Of these possibilities, the group velocity seems to be a good compromise, because it guarantees that the energy in the seismograms evaluated for the original and the EMP models arrives at the same time. Matching only the phase velocities of the original and the EMP models does not give as good a match of the seismograms. Matching only the eigenfunctions causes significant travel-time errors, and it is much more expensive.

The discrepancy (time delay of the wave traveling with $v_{gL}^{or}(T)$) due to the propagation effect can be estimated from the difference in the two corresponding maximum energy arrivals evaluated for the original and the EMP vertical profiles:

$$\Delta t = \frac{x}{v_{gL}^{EMP}(T)} - \frac{x}{v_{gL}^{or}(T)} = t_{prop}\frac{v_{gL}^{EMP}(T) - v_{gL}^{or}(T)}{v_{gL}^{or}(T)}.$$

Here $t_{prop} = x / v_{gL}^{EMP}(T)$. The time discrepancy between arrivals of the corresponding waves (groups of energy) for a given distance x will increase with larger relative error of the group velocity and longer time of wave propagation in the modified model t_{prop}. For a given period we may estimate the time for which the seismograms should match by

$$t_{prop} < T\frac{v_g^{or}(T)}{v_g^{new}(T) - v_g^{or}(T)}. \quad (3)$$

The effects due to source depth, receiver depth, and source radiation pattern are important if the Love- or Rayleigh-wave eigenfunctions of the original and the EMP models differ significantly at the source or receiver positions. The distortion of eigenfunctions due to a velocity change at shallow depths rapidly decays with depth. We have found numerically that the differences in eigenfunctions due to the receiver or source position at the free surface are also negligible. However, if a receiver or a source is situated inside the modified layer of the EMP model, the eigenfunctions of the EMP and the original models may differ significantly, thus causing some discrepancies.

A low-velocity layer in the model should not be eliminated if it can trap seismic waves within the frequency range of interest. We have numerically found that the lowest group velocity (the minimum of the Airy phases [Airy phase is a phase traveling with velocity for which group velocity has a local extreme]) is very sensitive to a minimum velocity near the surface. Therefore, the near-surface low velocity can be increased only if the frequency range of interest does not contain the frequency of the group velocity minimum. Furthermore, we have found that frequencies for which the higher mode velocities are real are usually higher than or near the frequency of the minimum of the group velocity of the fundamental mode. Consequently, we do not include group and phase velocities of higher modes in algorithm.

It is also important to include a search over the density. The best-fitting homogeneous layer of the EMP model tends to be of lower density compared with the original model. If we do not include a search over density, eigenfunctions of the EMP vertical profile would not match the eigenfunctions of the original model. The lower densities compensate for the increased velocity by maintaining the impedance contrast at the depth H of the replacement layer.

Equivalent Medium Parameters for a 3D Isotropic Model

To modify a 3D model we horizontally discretize it to be a set of 1D vertical profiles. We evaluate the group ve-

locity of the Love and Rayleigh waves in all 1D vertical profiles and find the minimum group velocity in the frequency range of interest. This minimum determines the mesh size of our numerical simulation. Vertical profiles with velocities lower than the minimum are modified with the algorithm described in the previous section. The limits of this approximation are analyzed in this section.

Algorithm for a 3D Isotropic Model

The input parameters of the algorithm are a 3D model of *P*-wave and *S*-wave velocities ($v_p^{or}(x,y,z)$ and $v_s^{or}(x,y,z)$, respectively) and density ($\rho^{or}(x, y, z)$) and the period range of interest (T_1, T_2).

In the first step, we discretize the original model to a finite set of vertical profiles at points $\{x_i, y_i, 0\}$. The horizontal discretization should be fine enough to capture the slowest regions of the original model. Then, we compute the group velocities of the Love $v_{gL}^{or}(T,x_i,y_i,0)$ and Rayleigh $v_{gR}^{or}(T,x_i,y_i,0)$ waves within the frequency range of interest at every point $\{x_i, y_i, 0\}$. The values of the group velocities must be independent of the discretization of the original model. We find the minimum

$$v_{\min} = \min_{T\in(T_1,T_2),x_i,y_i,0}(v_{gL}^{or}(T,x_i,y_i,0), v_{gR}^{or}(T,x_i,y_i,0)).$$

This determines the minimum velocity that must be used for the numerical simulation, which then sets the mesh size.

Now we again search through the entire original discretized model by examining vertical profiles for every point $\{x_i, y_i, 0\}$. If for a vertical profile $\{x_i, y_i, z\}$, the velocity does not drop below the minimum velocity $v_{\min}$, we do not modify that vertical profile, and parameters in the EMP model are equal to the original model for that profile. If for a vertical profile $\{x_i, y_i, z\}$, the velocity drops below the minimum velocity $v_{\min}$, we use the algorithm described in previous section with threshold value $v_{\min}$ to rediscretize that profile.

Discussion of the Algorithm for a 3D Isotropic Model

The algorithm is suitable for a heterogeneous model with weak lateral inhomogeneity near the surface as for instance defined by Levshin *et al.* (1989). The condition of the weak lateral inhomogeneity is locally satisfied by models with as much heterogeneity as the Southern California Velocity Model (SCVM) (Magistrale *et al.,* 2000). Figure 4 shows the Love-wave group velocities computed for a period of 3 sec for the SCVM (Version 2.2). Several authors (Graves, 1995; Olsen *et al.,* 1995; Olsen and Archuleta, 1996; Wald and Graves, 1998) have noted that the surface waves form the coda in their numerical simulations of the wave propagation inside the basins. This observation can be explained by the large zones of weakly heterogeneous group velocities in the basin regions as can be seen in Figure 4. The boundaries of the basins trap the surface waves inside the basins. Our algorithm finds a new model in which the group velocities for the periods of interest match the original model and preserves the heterogeneity of the original model. In contrast to a simple velocity clamping, the method we propose preserves the average velocity. This means that we increase the velocity in some regions of the original model as well as decrease it in other regions of the original model. The volumetric averaging of slowness (Muir *et al.,* 1992; Moczo *et al.,* 2000) is the most appropriate method to discretize an isotropic model to an isotropic model.

Numerical Tests

In order to test the method, we compare synthetic seismograms computed for the original and the EMP models. Tests with simple models will enable us to analyze the effects of the approximations we use. We start with the case of a layer over a half-space, test a complex vertically heterogeneous vertical profile selected from a realistic 3D model, and finally show how the method works for laterally heterogeneous models.

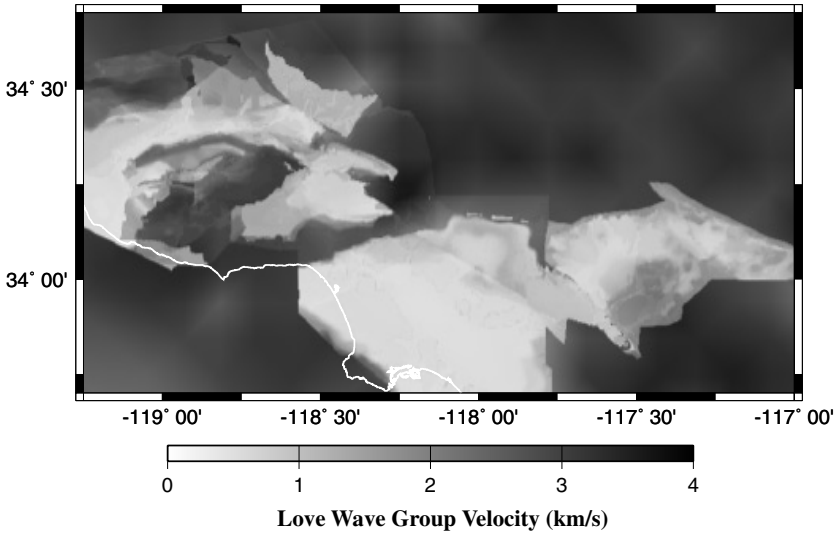

Figure 4. This figure shows the map of the Love-wave group velocities for a period of 3 sec, computed for the SCVM (Version 2.2, Magistrale *et al.,* 2000). The group velocities were computed at horizontal points (grid-spacing length 300 m) by taking a vertical velocity profile with medium parameters discretized every 25 m for the top 1000 m and then with increased spacing down to a depth of 45,000 m.

Table 1
Medium Parameters of the Three-Layer over the Half-Space Models

Models	Thickness (m)	β (m/sec)	α (m/sec)	ρ (kg/m^3)
Original Model	300.0	500.0	1000.0	1900.0
	∞	1000.0	1700.0	2200.0
EMP Model	500.0	640.0	1250.0	1430.0
	∞	1000.0	1700.0	2200.0
Velocity-Clamped Model	300.0	640.0	1250.0	1430.0
	∞	1000.0	1700.0	2200.0

For the case of a layer over the half-space we have chosen a layer with a velocity contrast of a factor of 2 to generate synthetic seismograms with observable dispersion. To test a large number of source locations in this model, we used the reciprocity method (Eisner and Clayton, 2001) with a single receiver at the free surface and 155 double-couple point sources located throughout the model. The test for variable source depth is more sensitive to a change in the eigenfunctions with depth, as certain combinations of eigenfunctions may be excited by the source mechanism. The source locations vary from 0 to 24 km of epicentral distance and from 0 to 3 km of depth. Generally, the deeper the source location, the smaller the effect of the near-surface velocity variations. Sources beyond an epicentral distance of 24 km were not tested because we limited our comparison to the first 60 sec. The time limit chosen here corresponds to the time set by the criterion for t_{prop} (see equation 3). The synthetic seismograms were compared for three source mechanisms from which a response due to an arbitrary double-couple mechanism can be evaluated by linear superposition (strike slip, vertical dip slip, and 45° dip slip). The original, the EMP, and the velocity-clamped models are described in Table 1. The EMP model was evaluated for a signal with energy at

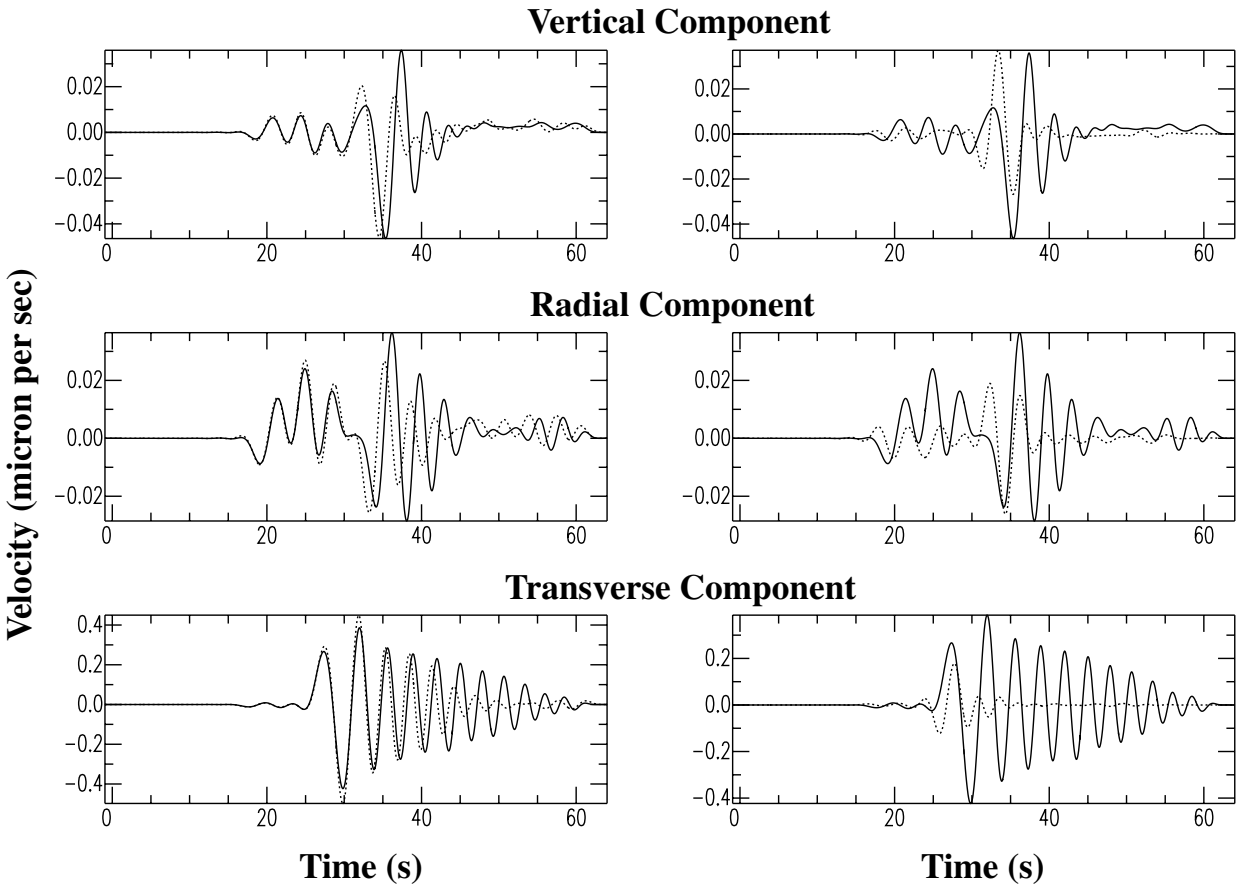

Figure 5. Comparison of the synthetic seismograms computed for the original, the EMP, and the velocity-clamped models. Three components of velocity (in μm/sec) due to a 45° dip-slip double-couple point source situated at the free surface (azimuth 90°, strike 90°, dip 90°, rake 45°, moment M_w 1.0). The epicentral distance is 24 km. In both columns, the solid line is the synthetic seismogram computed for the original model. The dashed line in the left column is the synthetic seismogram computed for the EMP model, whereas in the right column it shows synthetic seismograms computed for velocity-clamped model. The models are described in Table 1. All seismograms were low-pass filtered for periods longer than 3 sec.

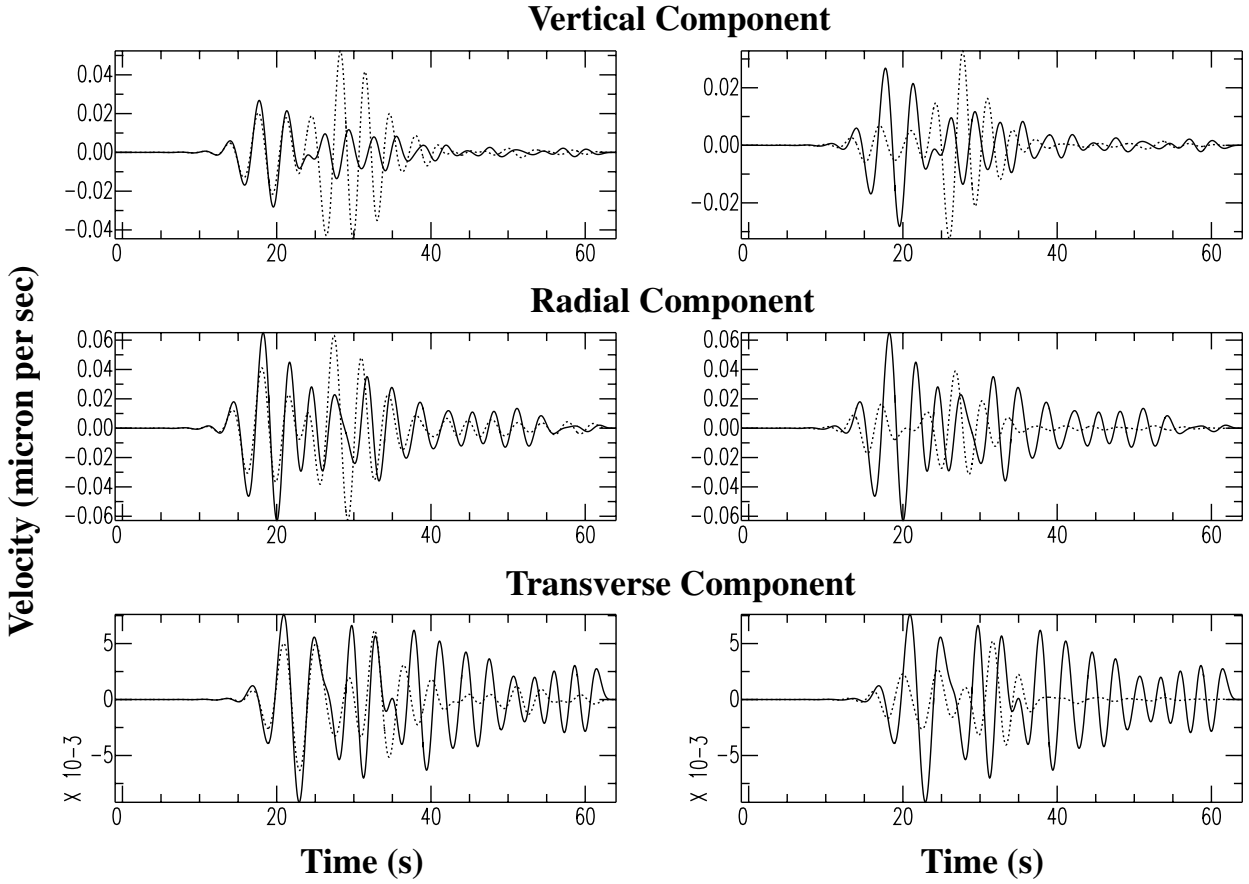

Figure 6. Comparison of the synthetic seismograms computed for the original, the EMP, and the velocity-clamped models: three components of velocity (in μm/sec) due to a dip-slip double-couple point source situated 0.25 km below the free surface (azimuth 90°, strike 0°, dip 90°, rake 90°, moment M_w 1.0). The epicentral distance is 22 km. See Figure 5 for more details.

periods of 3 sec and longer. To compare models with equal numerical cost of computation, the velocity-clamped and the EMP models have the same minimum velocities.

Figure 5 shows the worst matching seismograms (EMP and original) computed with a finite-difference technique using velocity-stress formulation solved by a staggered-grid scheme with fourth-order accuracy in the spatial derivatives and second-order accuracy in time derivatives. The seismograms were computed for the original, the EMP, and the velocity-clamped models. We have used a triangular source time function with a length of 3 sec, and the model was discretized at 10 points per minimum *S*-wave wavelength to avoid the numerical dispersion (dx = 0.15 km). The worst matching seismograms as determined by cross correlation were selected from 465 (155 source positions and three mechanisms) source-receiver combinations. The relative Love-wave group velocity error corresponding to a period of 3.0 sec is 7.5%, and criterion (3) sets t_{prop} to be less than 40.0 sec. The EMP and the seismograms of the original model agree within a line thickness up to 30 sec, and the agreement deteriorates for arrivals after 45 sec on the transverse component. The agreement of the radial and vertical components deteriorates for arrivals after approximately 37 sec; however, the amplitude of these arrivals is an order of magnitude smaller than the amplitude on the transverse component. The velocity clamping does a poor job for all times after the onset. Also note that both the source and the receiver are situated at the free surface on the top of the modified layer, which means that changes in the eigenfunctions due to the modified medium parameters do not affect the synthetic seismograms for EMP vertical profile.

Figure 6 shows the poorest matching seismograms computed for the original, the EMP, and the velocity-clamped models with a double-couple point source mechanism of 90° dip slip situated 0.25 km below the free surface at an epicentral distance of 22 km. Seismograms computed for the original and the EMP agree well up to 25 sec, and the agreement deteriorates for both the phase and the amplitude for times 25–40 sec on all components. The source is situated at the center of the modified layer (thickness 0.5 km), and at this depth the eigenfunctions of the original and the EMP models (and the velocity-clamped model) may significantly

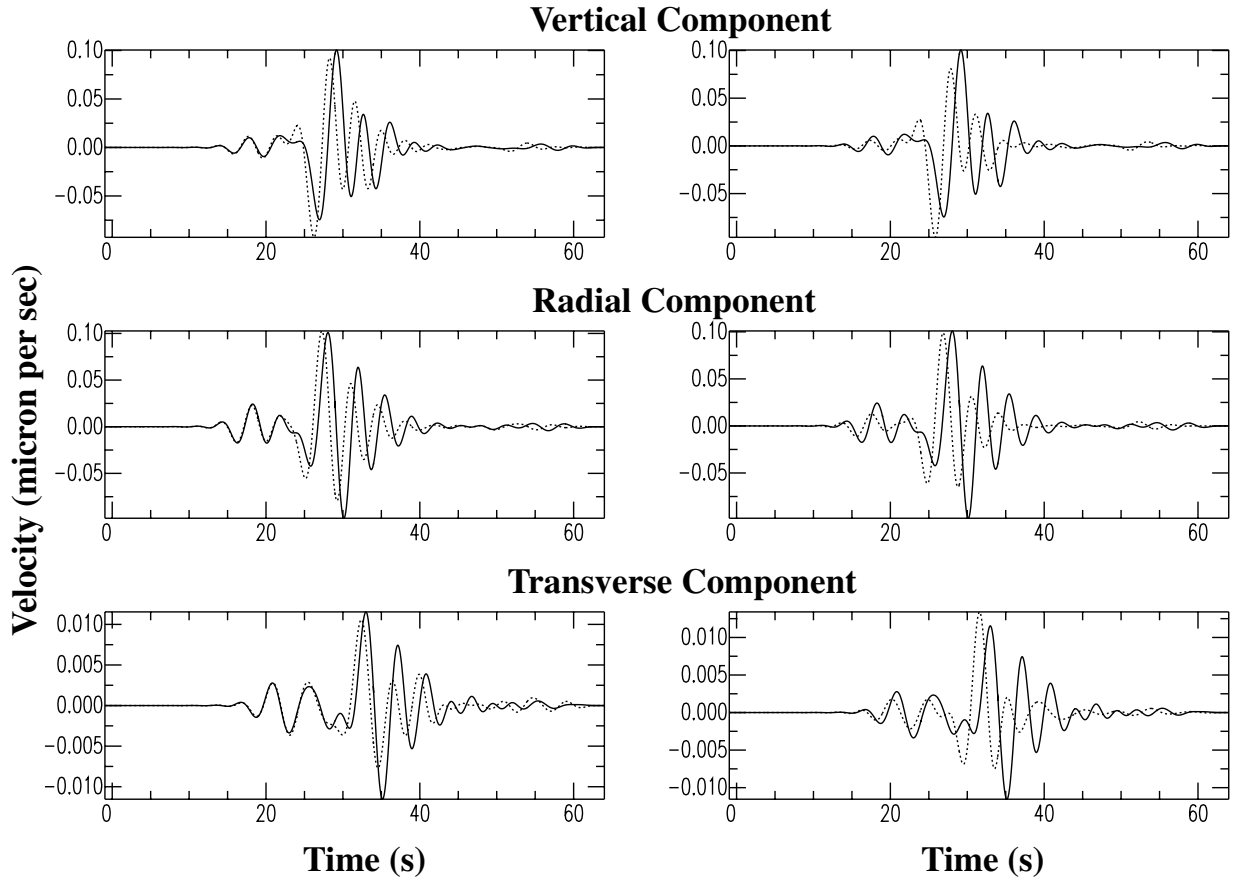

Figure 7. Comparison of the synthetic seismograms computed for the original, the EMP, and the velocity-clamped models. Three components of velocity (in microns per second) due to a dip-slip double-couple point source situated 2.0 km below the free surface (azimuth 90°, strike 0°, dip 90°, rake 90°, moment M_w 1.0). The epicentral distance is 22 km. See Figure 5 for more details.

differ. Since we did not observe a similar discrepancy (as in Fig. 6) for different source mechanisms at the same hypocenter, we infer that it is not caused by the epicentral distance but by the source mechanisms, which increase the difference between the eigenfunctions of the original and EMP models. To further test this hypothesis, we compared seismograms due to deeper sources for which the eigenfunctions do not differ as much between the original and the EMP models. Figure 7 shows seismograms due to the same double-couple point source mechanism, the same epicentral distance, but at a depth of the source 2 km. The seismograms computed for the original and the EMP models match well up to 40 sec, except the transverse component, which is 10 times smaller than the other two components, and therefore a small discrepancy on the other two components may project into a large discrepancy on the transverse component. Again, the simple clamping of the minimum velocities produces a much worse result.

Figure 8 gives the medium parameters and the dispersion curves for a single vertical profile in the Los Angeles basin from the SCVM (Version 2.2, Magistrale *et al.,* 2000). The near-surface sedimentary layer causes a sharp drop in all medium parameters with the minimum velocity reaching 250 m/sec. The dispersion curve of the Love-wave group velocity shows three Airy phases at 0.15 sec, 2.6 sec, and 3.1 sec. As discussed previously, we cannot increase the minimum velocity in the model if the group velocities of the period range of interest contain the overall minimum of the Love-wave group velocity (T = 0.15 sec). We have modified the original model for signals with energy at 3 sec and higher periods to have a minimum velocity of 700 m/sec. The relative error of the Love-wave group velocity caused by the increased minimum velocity is 5.7% for the period of 3 sec; therefore, by equation (3), the seismograms should agree up to 52 sec.

Synthetic seismograms for a shallow source (1 km deep) computed for the original, the EMP, and the velocity-clamped models are compared in Figure 9. We computed the synthetic seismograms with the Thompson–Haskell propagator matrix method (Thompson, 1950; Haskell, 1953). We tested and compared a large number of source mechanisms, epicentral distances, and source depths (the re-

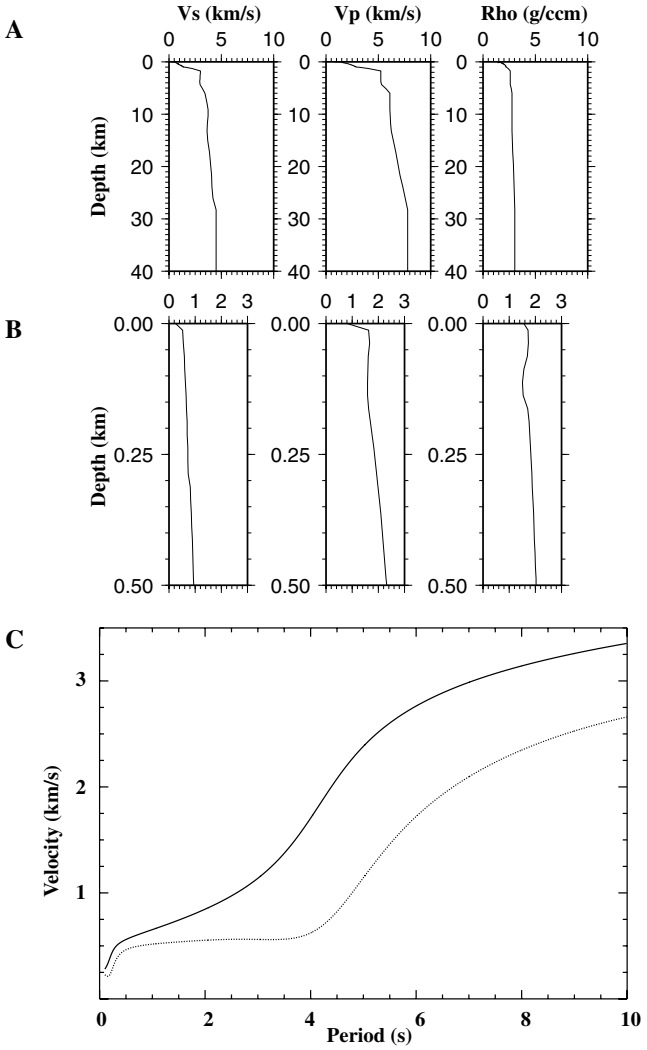

Figure 8. Medium parameters and dispersion curves of the vertical velocity profile selected from the SCEC velocity model Version 2 (Magistrale *et al.,* 2000) at 33.94° N and 118.15° W. (A) Profiles showing dependency of the *S*-wave velocity (Vs), *P*-wave velocity (Vp), and density (Rho) on depth. (B) The three graphs show details of medium parameter profiles for the top 0.5 km. (C) The graph shows the dispersion of the Love-wave phase (solid line) and Love-wave group (dashed line) velocities. Note the Airy phases at 0.15 sec, 2.6 sec, and 3.1 sec.

ceiver was fixed at the free surface), and this example represents an average fit between the seismograms computed for the original, the EMP, and the velocity-clamped models. The Airy phase arrival on the transverse component is at approximately 55 sec (theoretical arrival time of 53.5 sec). The synthetic seismograms computed for the original and the EMP models agree very well, even for times greater than the predicted 52 sec. The Airy phase is poorly matched by synthetic seismograms computed for the velocity-clamped model. The value of the clamping velocity was estimated from the EMP solution itself and leads to a similar result. However, if the clamping velocity has been chosen at higher values, the results would be substantially different.

Finally we tested the method for a simple 3D heterogeneous medium. We chose a model similar to the microbasin model of figure 10 of Saikia *et al.* (1994), who pointed out the importance of the near-surface low-velocity zones for full waveform seismograms. Our 3D model is shown in Figure 10. The *S*-wave velocity drops to 0.2 km/sec in the original model. The equivalent medium parameter model has a minimum velocity of 0.5 km/sec, and the relative group velocity error caused by this model modification is 0.4% for the period of 3 sec. Therefore, we may expect our seismograms to agree upto 750 sec. We use a rectangular shape of the basin model to avoid effects due to a different discretization for the finite-difference grid. The grid for the EMP model ($dx = 0.25$ km) is almost twice as coarse as the grid of original model ($dx = 0.15$ km).

We simulated the synthetic seismograms at a receiver situated at the free surface from 384 point sources for three different source mechanisms (strike slip, 90° dip slip, and 45° dip slip). Figure 11 shows the synthetic seismograms with the lowest cross-correlation coefficient. The late arrivals (20–30 sec) are caused by trapped energy in the basin. The seismograms from the original and the EMP models match within a line thickness. The perfect match of the multiply reflected waves inside the low-velocity region demonstrates the capability of the method to handle sedimentary basins. The numerical simulation for the EMP model required 8 times less computation time and 4 times less computer memory than with the original model.

Conclusions

Figure 1 shows that the synthetic seismograms are significantly dependent on the *a priori* chosen value of the clamping velocity. The misfit between synthetic seismograms computed in original and clamped velocity models can be quite significant, particularly if one is using late-arriving energy. The differences between the Love-wave group velocities in the original and modified models are used to estimate the misfit between seismograms computed in the original and modified models. By matching the Love-wave group velocities we are able to change the original model to the one with higher minimum velocity and still minimize the discrepancy between the seismograms computed in the original and modified models.

The synthetics computed for the models with the equivalent medium parameters produce a significantly better match to the original models than the synthetics computed for the velocity-clamped models. This allows a significant reduction in model size and computational time required. For the 3D velocity model shown here, the computational time was reduced by a factor of 8 and the memory requirements by a factor of 4. Tests also show that the t_{prop} time of equation (3) does a good job of predicting the amount of time that the solution will be relatively free of artifacts.

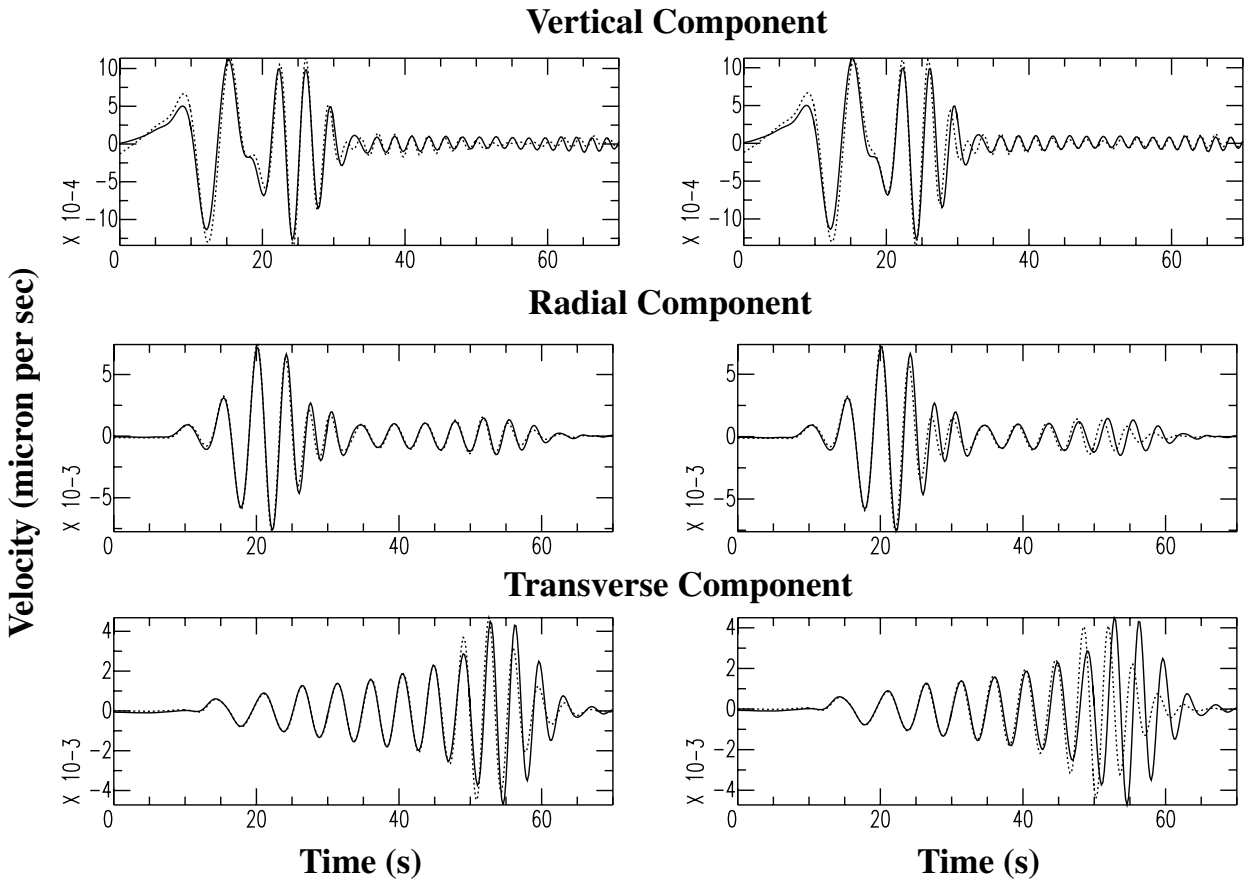

Figure 9. Comparison of the synthetic seismograms computed for the original, the EMP, and the velocity-clamped models for complex vertical profile. Three components of velocity (in microns per second) due to a strike-slip double-couple point source situated 1.0 km below the free surface (azimuth 40°, strike 0°, dip 90°, rake 0°, moment M_w 1.0). The epicentral distance is 30.0 km. In both columns, the solid line is the synthetic seismogram computed for the original model of Figure 8. The dashed line in the left column is the synthetic seismograms computed for the EMP model of minimum velocity 0.7 km/sec, whereas in the right column it shows synthetic seismograms computed for velocity-clamped model at 0.7 km/sec. All seismograms were low-pass filtered for periods longer than 3 sec.

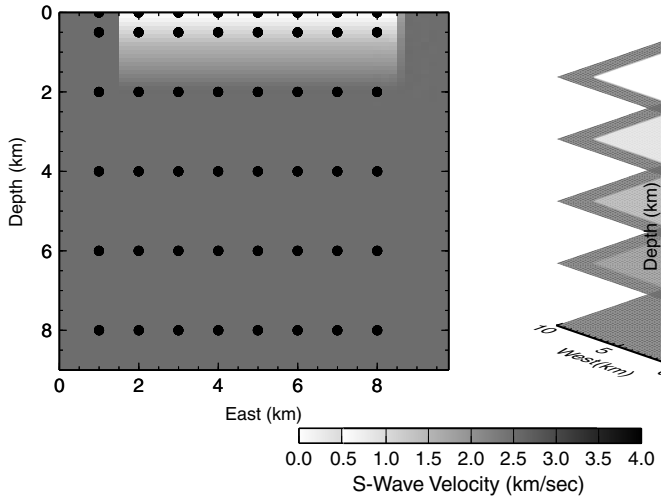

Figure 10. The 3D heterogeneous model used for the 3D test. The left plot shows *S*-wave velocity in the east-depth plane in the center of the model. The black circles represent positions of sources projected on the plane. The right plot illustrates the 3D structure of the rectangular basin. The black circle at the top represents the position of the receiver.

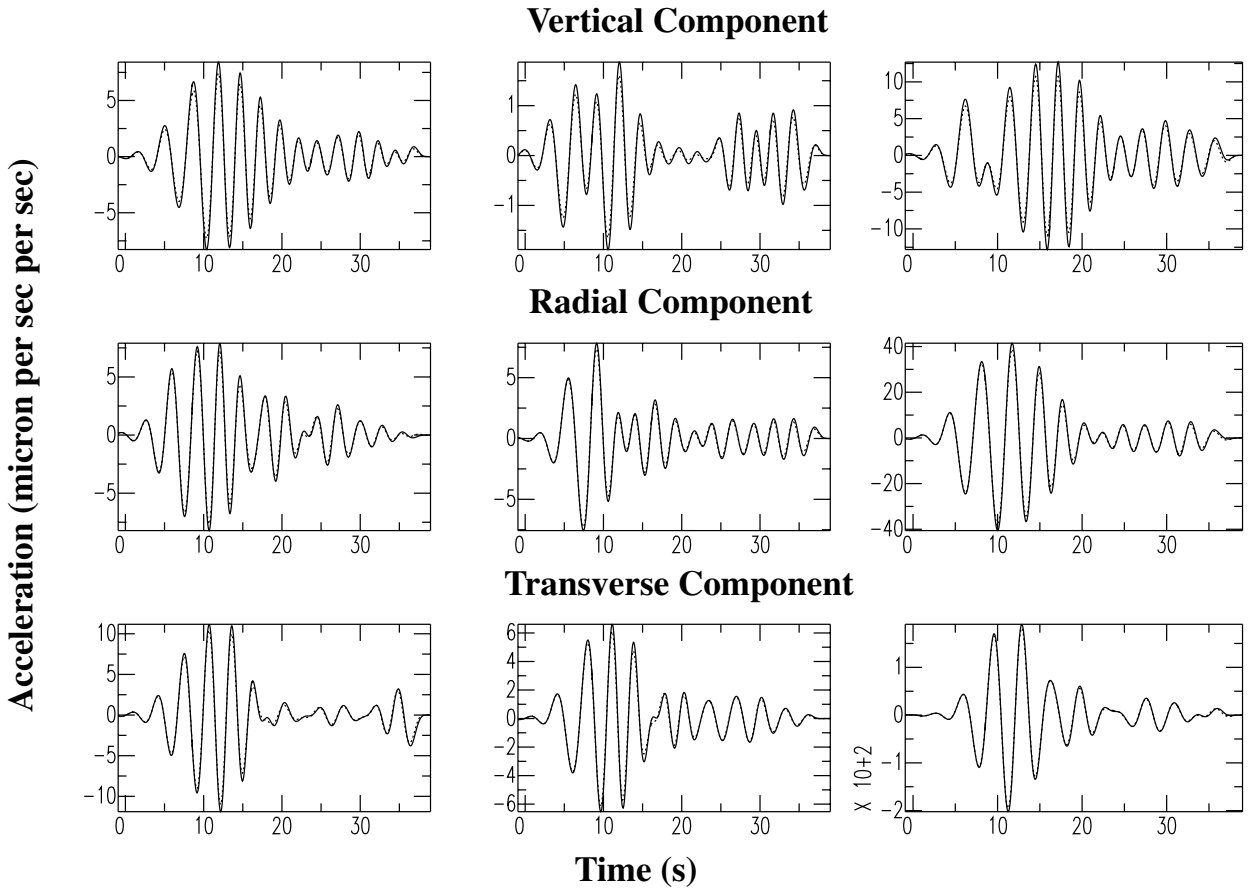

Figure 11. Comparison of the synthetic seismograms computed for the original and the EMP for a 3D model. Three components of acceleration (in microns per second per second) due to three double-couple point sources: 90° dip slip (strike 0°, dip 90°, and rake 90°) (left column), 45° dip slip (strike 0°, dip 45°, and, rake 90°) (middle column), and strike slip (strike 0°, dip 90°, and rake 0°) (right column). The synthetic seismograms were computed for the model shown in Figure 10. The receiver was situated at the surface at 0.5 km east and 0.5 km north of the edge of the basin. The source for 90° dip slip and 45° dip slip was situated at a depth of 0.5 km, and it was 3.5 km north and 0.5 km west of the edge of the basin. The source for the strike-slip point source is at the free surface 5.5 km north and 5.5 km east of the edge of the basin. The solid line represents synthetic seismograms computed for the original model described in Figure 10. The dashed line represents synthetic seismograms computed with equivalent medium parameters with a minimum velocity 0.5 km/sec. All seismograms were low-pass filtered for periods longer than 3 sec.

Acknowledgments

The authors are grateful to Luis Rivera for interesting insights during the development of this method. Special thanks go to Hiroo Kanamori who not only followed our progress but significantly helped with the determination of the error criterion. Dimitri Komatitsch greatly helped to make this manuscript readable and offered his experience to evaluate one of the numerical tests used in this article. We thank Václav Vavryčuk, Kim Olsen (reviewer), Ivan Pšenčík, Jeroen Tromp, Jascha Polet, Si-Dao Ni, John Etgen, and anonymous reviewer for their input when developing this method and preparing the manuscript. Many of the figures were made with Generic Mapping Tools software (Wessel and Smith, 1991). This research was supported by the Southern California Earthquake Center (SCEC). The SCEC is funded by NSF Cooperative Agreement EAR-8920136 and U.S. Geological Survey Cooperative Agreements 14-08-0001-A0899 and 1434-HQ-97AG01718. The SCEC Contribution Number for this article is 524. This is Contribution Number 8820 from the Division of Geological and Planetary Sciences, California Institute of Technology.

References

Aki, K., and P. Richards (1980). *Quantitative Seismology,* W. H. Freeman, New York.

Backus, G. E. (1962). Long-wave elastic anisotropy produced by horizontal layering, *J. Geophys. Res.* **67,** 4427–4440.

Eisner, L., and R. W. Clayton (2001). A reciprocity method for multiple source simulations, *Bull. Seism. Soc. Am.* **91,** 553–560.

Graves, R. W. (1995). Preliminary analysis of long-period basin response in the Los Angeles region from the 1994 Northridge earthquake, *Geophys. Res. Lett.* **22,** 101–104.

Graves, R. (1996). Simulating seismic wave propagation in 3D elastic me-

dia using staggered-grid finite differences, *Bull. Seism. Soc. Am.* **86,** 1091–1106.

Graves, R. (1997). Effects of small scale near surface geologic heterogeneity on strong ground motions at long periods (T > 1 sec), *Seism. Res. Lett.* **68,** 302.

Graves, R. (1998). Three-dimensional finite-difference modeling of the San Andreas fault: source parameterization and ground-motion levels, *Bull. Seism. Soc. Am.* **88,** 881–897.

Haskell, N. (1953). The dispersion of surface waves on multilayered media, *Bull. Seism. Soc. Am.* **43,** 17–34.

Komatitsch, D., and J. Tromp (1999). Introduction to the spectral-element method for three-dimensional seismic wave propagation, *Geophys. J. Int.* **139,** 806–822.

Levshin, A., T. Yanovskaya, A. Lander, B. Bukchin, M. Barmin, L. Ratnikova, and E. Its (1989). *Seismic Surface Waves in a Laterally Inhomogeneous Earth,* Vol. 1. Kluwer, Hingham, Massachusetts.

Magistrale, H., S. Day, R. Clayton, and R. Graves (2000). The SCEC Southern California reference 3D seismic selocity model Version 2, *Bull. Seism. Soc. Am.* **90,** S65–S76.

Magistrale, H., K. McLaughlin, and S. Day (1996). A geology-based 3D velocity model of the Los Angeles basin sediments, *Bull. Seism. Soc. Am.* **86,** 1161–1166, *http://www.scecdc.scec.org/3Dvelocity/3Dvelocity.html.*

Moczo, P., E. Bystricky, J. Kristek, J. Carcione, and M. Bouchon (1997). Hybrid modeling of P-SV seismic motion at inhomogeneous viscoelastic topographic structures, *Bull. Seism. Soc. Am.* **87,** 1305–1323.

Moczo, P., J. Kristek, and R. Archuleta (2000). 3d 4th-order displacement scheme: a new scheme sensitive to heterogeneity of a medium, *EOS* **81,** F848.

Muir, F., J. Dellinger, J. Etgen, and D. Nichols (1992). Modeling elastic fields across irregular boundaries, *Geophysics* **57,** 1189–1193.

Olsen, K. (2000). Site amplification in the Los Angeles basin from three-dimensional modeling of ground motion, *Bull. Seism. Soc. Am.* **90,** 677–685.

Olsen, K., and R. Archuleta (1996). Three-dimensional simulation of earthquakes on the Los Angeles fault system, *Bull. Seism. Soc. Am.* **86,** 575–596.

Olsen, K., R. Archuleta, and J. Matarese (1995). Magnitude 7.75 earthquake on the San Andreas fault: three-dimensional ground motion in Los Angeles, *Science* **270,** 1628–1632.

Olsen, K., R. Madariaga, and R. Archuleta (1997). Three-dimensional dynamic simulation of the 1992 Landers earthquake, *Science* **278,** 834–838.

Opršal, I., and J. Zahradník (1999). Elastic finite-difference method for irregular grids, *Geophysics* **64,** 240–250.

Saikia, C., D. Dreger, and D. Helmberger (1994). Modeling of energy amplification recorded within greater Los Angeles using irregular structure, *Bull. Seism. Soc. Am.* **84,** 47–61.

Schoenberg, M., and F. Muir (1989). A calculus for finely layered anisotropic media, *Geophysics* **54,** 581–589.

Thompson, W. (1950). Transmission of elastic waves through a stratified solid medium, *J. Appl. Phy.* **21,** 89–93.

Wald, D., and R. Graves (1998). The seismic response of the Los Angeles basin, California, *Bull. Seism. Soc. Am.* **88,** 337–356.

Wessel, P., and W. Smith (1991). Free software helps map and display data, *EOS* **72,** 441.

1200 California Blvd. 252-21
Pasadena, California 91106
leisner@cambridge.scr.slb.com

Manuscript received 1 April 2001.